APPLICATION OF OPTIMIZATION TECHNIQUES AND THE ENTHALPY METHOD FOR SOLVING A 3D-INVERSE PROBLEM DURING A TIG WELDING PROCESS

Cristiene Vasconcelos Gonçalves, cristiene@prove.ufu.br
Solidonio Rodrigues Carvalho,srcarvalho@mecanica.ufu.br
Gilmar Guimarães, gguima@mecanica.ufu.br

Av. João Naves de Ávila, 2160 - Campus Santa Mônica - Bloco 1M - Uberlândia/MG

Abstract. *Tungsten inert Gas (TIG) is a welding process that takes place in an atmosphere of inert gas and uses a tungsten electrode. In this process the heat input identification is a complex task and represents an important rule in the optimization of the welding process. The technique used to estimate the heat flux is based on solution of inverse three-dimensional transient heat conduction model with moving heat sources. In this sense the thermal fields at any region of the plate or at any time are determined from the estimation of the heat rate that is delivered to the workpiece. The direct problem is solved by an implicit finite difference method. The system of linear algebraic equations is solved by Successive Over Relaxation method (SOR) and the inverse problem is solved using the Golden Section technique. The golden section techniques minimizes a square error function that is based on the difference of theoretical and experimental temperature. The temperature measurements are obtained by using thermocouples on accessible regions of the workpiece surface while the theoretical temperatures are calculated from the 3D transient thermal model.*

Keywords*: entalpia, mudança de fase, secção áurea, problemas inversos, soldagem.*

1. INTRODUCTION

Welding processes that involve material phase change are used in a large number of metallic structures such as buses, airplanes, reactors or oil ducts. Once these structures have acquired a high level of safety, the manufacturing processes, in special welding, must be carefully considered. TIG is one of the most widely employed welding processes that are applied with success for welding of stainless steels and non-ferrous materials. In this process, a tungsten electrode is shielded by a flow of inert gas such as argon (normally employed), helium, nitrogen, hydrogen or mixtures. The union of two or more workpieces is obtained through a voltaic arc which is a moving intense heat source.

The analysis of the thermal behavior of the physical phenomenon that takes place in the process is crucial to understand, for example, the width and depth of weld penetration, the microstructure changes in the base metal thermally affected or the residual stress that appear in the welding process.

One requisite to determine the temperature field in the presence of welding process is to know the real heat flux waste or the geometry and interface position of weld pool present in the process. Once known these parameters, a direct problem is established and the temperature field can, then, be calculated.

Transient heat transfer problems involving melting or solidification, such as is the problem due to a TIG welding process, are usually referred to as phase-change or moving-boundary problems. The solution of such problems is inherently difficult because the interface between the solid and liquid phases is moving as the latent heat is absorbed or released at the interface. As a result, the location of the solid-liquid interface is not known a priory and must follow as a part of the solution (Crank, 1984). One requisite to determine the temperature field under welding processes is to know either the actual heat flux or the geometry and interface position of weld pool. Once these parameters are known, a direct problem is established and the temperature field can, then, be calculated. Several pieces of work, analytical (Rosenthal (1941), Tsai and Hou (1988), Nguyen et. al (1999)) or numerical (Bonifaz (2000), Voller and Prakash (1987) and Al-Khalidy (1995)) that deals with this direct problem can be found in the literature. Besides the hypothesis of knowing the heat flux, important phenomena like metallic phase changes, thermal properties dependence on the temperature or heat losses by convection or radiation are neglected or considered known. However, the identifications of heat flux or the weld pool geometry and position are not trivial in a real welding. The main difficulty, in this case, is that these parameters are not reliable available or they are not so easily measured directly. A mean of overcoming this difficulty is to use inverse techniques. However, the majority of work that deals with inverse problem techniques in welding problems (Al-Khalidy (1997), Rubinsky and Shitzer (1978), Hsu et. al. (1986)) just uses simulated studies. Thus, the main goal of this work is to contribute to the welding related studies on heat flux and temperature field by presenting a solution based on inverse technique applied to the TIG process.

This work tries to improve previous research presenting a procedure to solve a inverse three-dimensional transient heat conduction model with moving heat sources. The thermal fields at any region of the plate or at any time are determined from the estimation of the heat rate that is delivered to the workpiece. The direct problem is solved by an implicit finite difference method. The system of linear algebraic equations is solved by Successive Over Relaxation method (SOR) and the inverse problem is solved using the Golden Section technique. The model developed is based on enthalpy method described by Al-Khalidy (1997) that is applied in a two-dimensional model.

2. DIRECT PROBLEM

2.1. Moving-boundary problem formulation

Figure 1 presents the transient heat transfer problems involving phase change due to a TIG welding process in a AISI 304 sample. The moving-boundary problem can, then, be described by diffusion equation considering a three-dimensional system and nonlinear temperature-dependent thermal conductivity $k(\theta)$ and specific heat $c(\theta)$ in the solid region as

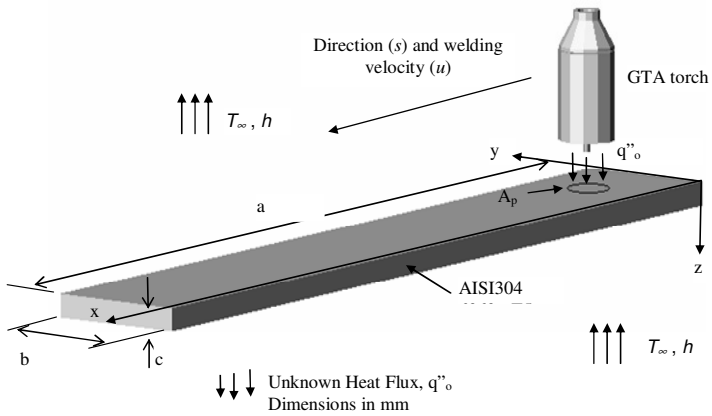

Figure 1. Schematic representation of the three-dimensional thermal welding process.

$$\frac{\partial}{\partial x}\left(k(T)\frac{\partial T}{\partial x}\right)+\frac{\partial}{\partial y}\left(k(T)\frac{\partial T}{\partial y}\right)+\frac{\partial}{\partial z}\left(k(T)\frac{\partial T}{\partial z}\right)=\rho C(T)\frac{\partial T}{\partial t} \tag{1}$$

subjected to the following boundary conditions:

in the regions exposed to the environment

$$-k_i\frac{\partial T}{\partial \eta}=h_i(T-T_\infty) \tag{1b}$$

and at the region of heat suplied

$$-k_i\frac{\partial T}{\partial \eta}=q_0^{"}(t) \tag{1c}$$

where $\partial/\partial\eta$ denotes differentiation along the outward-drawn, normal to the boundary surface S, h_i is the heat transfer coefficient, T_∞ is the ambient temperature and q_0" is a moving point of heat source of constant strength q_p (W), that releases its energy continuously over the time as it moves with a constant velocity u in the positive x direction.

It should be noted in Fig. (1) that all surfaces are exposed to the environment but the area of heat suplied, A_p. As mentioned before, this area is subjected to the heat flux q_0" generated welding , Fig. (1b).

Equation (1) refers to fixed coordinated system *(x,y,z)*. However, depending on the value of the power supply a fusion zone in the region where the heat is delivered can occur. In this case, Eq. (1) must consider a region R of pure material separated into liquid region liquid region, R_l, and solid region, R_s . The two region is separated by an interface$\Re$.

Thus, two equations must be written independently (Al-Khalidy, 1997). One for solids state,

$$\frac{\partial}{\partial x}\left(k_s\frac{\partial T_s}{\partial x}\right)+\frac{\partial}{\partial y}\left(k_s\frac{\partial T_s}{\partial y}\right)+\frac{\partial}{\partial z}\left(k_s\frac{\partial T_s}{\partial z}\right)=\rho C_s\frac{\partial T_s}{\partial t} \tag{2}$$

and the other for the liquid region

$$\frac{\partial}{\partial x}\left(k_l\frac{\partial T_l}{\partial x}\right)+\frac{\partial}{\partial y}\left(k_l\frac{\partial T_l}{\partial y}\right)+\frac{\partial}{\partial z}\left(k_l\frac{\partial T_l}{\partial z}\right)=\rho C_l\frac{\partial T_l}{\partial t} \tag{3}$$

The physical conditions that are valid for the interface are given by Stefan condition as:

$$\left(k\frac{\partial T}{\partial \eta}\right)_s - \left(k\frac{\partial T}{\partial \eta}\right)_l = \rho\lambda v \qquad and \quad T_s = T_l = T_m \tag{4}$$

where $\lambda = L$ during the solidification and $\lambda = -L$ during fusion. In Eq.(4) L represents the total latent heat of fusion.

The heat flux condition to the interface can be insert in Eqs.(2) and (3) using the enthalpy concept that take into account the temperature difference at interface. It means, *H(T)* is the enthalpy function defined by (Clank, 1984):

$$H(T) = \int_{T_o}^{T} \{\rho(\theta)C(\theta) + \rho(\theta)L\delta(\theta - T_m)\}d\theta \tag{5}$$

where T_0 is reference temperature lower than the fusion temperature T_m, and the specific calor C(T) is strongly dependent on temperature T.

Considering Eq.(5), Eq.s (2) and (3) can be written together as follows

$$\frac{\partial}{\partial x}\left(k(T)\frac{\partial T}{\partial x}\right) + \frac{\partial}{\partial y}\left(k(T)\frac{\partial T}{\partial y}\right) + \frac{\partial}{\partial z}\left(k(T)\frac{\partial T}{\partial z}\right) = \frac{\partial[\rho\, h(T)]}{\partial t} \tag{6}$$

and the interface condition can be rewritten by

$$T_1 = T_2 = T_m, \quad \left[k\frac{\partial T}{\partial n}\right]_1^2 = -\rho L v \ , \tag{7}$$

were the index i=1,2 denotes the two phase separated by a moving interface, *r=s(t).* Index 1 refers to solid phase whereas index 2 to the liquid phase.

In Eq.(9) the specific entalpy can be expreses by (Clank, 1984):

$$h(x, y, z, t, T) = f.L + C(x, y, z, t, T)(T(x, y, z, t, T) - T_{sat}) \tag{8}$$

where T_{sat} is the saturation temperature and f(x,y,z,t) the massic fraction of liquid phase that is given by

$$f(x, y, z, t, T) = \begin{cases} 0 & se \quad h(x, y, z, t, T) < 0 \\ \dfrac{h(x, y, z, t, T)}{L} & se \quad 0 \le h(x, y, z, t, T) \le L \\ 1 & se \quad h(x, y, z, t, T) \ge L \end{cases} \tag{9}$$

By substituting Eqs.(8) and (9) into Eq.(6) the thermal model based on enthalpy can be obtained by

$$\frac{\partial}{\partial x}\left(k\frac{\partial T}{\partial x}\right) + \frac{\partial}{\partial y}\left(k\frac{\partial T}{\partial y}\right) + \frac{\partial}{\partial z}\left(k\frac{\partial T}{\partial z}\right) + \ Q_m(x, y, z, t) = \frac{\partial(\rho C\, T)}{\partial t} \tag{10}$$

Thus, in Eq.(10) the phase change condition is isolated in a latent heat source term and is as follows

$$Q_m(x, y, z, t) = -\frac{\partial(\rho(f(x, y, z, t).L - C(x, y, z, t).T_{sat}))}{\partial t} \tag{11}$$

Equation (10) is subjected to the boundary conditions

$$k\frac{\partial T}{\partial \eta}\bigg|_{s=s_i} = h_i\left[T_{s=s_i} - T_\infty\right] \tag{12}$$

$$-\lambda_i\frac{\partial T}{\partial \eta} = q_0'' \tag{13}$$

and the initial condition

$$T(x, y, z, 0) = T_\infty \tag{14}$$

If the heat flux q_0" is known Equations (10-14) represent the direct problem that can be reduced to the solution of the linear algebraic equations system (equation 6) that is solved by using the Successive Over Relaxation method (SOR) (Patankar, S., 1980).

2.2 – Heat transfer coefficient obtaining, h_i

Due to the temperature gradients in the air and the gravitational field, buoyancy force will induce free convection currents around the sample. In this case, assuming that the gravitational force acts in axis z direction, the local convection coefficient h_i can be expressed as (Incropera et al., 2007),

$$h = \frac{Nu_l \; k_a}{L_c} \tag{15}$$

where Nu_l is the local Nusselt number, K_a is the thermal conductivity of the air and L_c is defined as the characteristic length of the sample.

Values of Nu_l and L_c will depend on the sample geometry. The characteristic length varies along the axis z in vertical heated surfaces and tends to zero in the center of the plan in horizontal heated surface (upper or down). Besides, in the horizontal surfaces L_c increases with x and y according to the expression:

$$L_c = \sqrt{\left(x - \frac{a}{2}\right)^2 + \left(y - \frac{b}{2}\right)^2} \tag{16}$$

Appropriate empirical correlation has been developed for common external flow geometries in order to calculate values for the Local Nusselt number Nu_l. The correlations for the each geometry can be summarized in case of free convection over a vertical heated surface by

$$Nu_l = 0.68 + \frac{0.67 Ra_l^{1/4}}{\left[1 + (0.492 / Pr)^{9/16}\right]^{4/9}} \qquad Ra_l \le 10^9 \tag{17}$$

where Ra_l is the Rayleigh number and Pr is the Prandtl number, and

$$Nu_l = 0.54 Ra_l^{1/4} \qquad 10^4 \le Ra_l \le 10^7 \tag{18}$$

$$Nu_l = 0.15 Ra_l^{1/3} \qquad 10^7 \le Ra_l \le 10^{11} \tag{19}$$

$$Nu_l = 0.27 Ra_l^{1/4} \qquad 10^5 \le Ra_l \le 10^{10} \tag{20}$$

for a free convection over the lower and upper surfaces on an heated horizontal surface respectively.

The use of Eqs. (17-20) in the direct thermal model allows Nu_l be calculated to any position on the plate and for each step of time. This procedure allows a transient analysis of the free convection along the aluminum surface during the welding process. The Nu_l profile for horizontal heated surface was compared with the literature values obtained from Pretot et al. (2000). It was verified a good agreement among the results.

2.3. Numerical solution of the direct problem

The Equations (10-16) are then discretized using a Cartesian mesh with 360000 grid points.

The irregular three-dimensional mesh is generated according to the aluminum plate dimensions and physical characteristics using a mesh generation algorithm (Carvalho, 2005).

The integration of Eq. (10) over the control volume for an internal node i and the integration of Eqs. (11-14) over the control volumes associated with the boundary nodes result in a system of equations that can be reduced to general form

$$a_i T_i = a_i^0 T^0 - \sum_n a_n T_n + b_i \tag{21}$$

where the subscripts i and n indicate the appropriate node point value and neighbor node points, respectively. The ***a*** and ***b*** coefficient depend on the thermal properties and numerical scheme. The a_i^0 is the unsteady coefficient at the preiuos time step. The ***b*** term represents the source term given by

$$b = Q_m + \frac{\rho . T_{sat} (C_P - C_P^0)}{\Delta t} \tag{22}$$

where

$$Q_m = -\frac{\rho L \left(f_P - f_P^0 \right)}{\Delta t} \tag{23}$$

The direct problem is then reduced to the solution of the linear algebraic equations system (Eq. 6) that is solved by using the Successive Over Relaxation method (SOR) with a relaxation coefficient $W = 1.95$.

2.3. Numerical solution of the inverse problem

One way to estimate the heat flux q_0", present in Eq. (1), is to require that the traditional least square function, F_q, defined as the error between the computed temperature T_i and the measured temperature Y_i be minimized with respect to the unknown $q(t)$. F_q is then defined as

$$F_q = \sum_{j=1}^{N} \sum_{i=1}^{M} \left(Y(\boldsymbol{r_n}, t_m) - T(\boldsymbol{r_n}, t_m, q_m) \right)^2 \tag{17}$$

where ***r*** represents the vector position of the rectangular coordinate system *(x,y,z), n* denotes the thermocouple position and *m* denotes the measurement time.

There are several inverse techniques that can solve this welding problem optimization. It can be cited, for example, sequential algorithms as the conjugate gradient with adjoint equation method (Alifanov , 1974), parameter estimation approach (Beck at al, 1985) or robustness techniques as simulated annealing method (Gonçalves, 2006). All techniques uses temperature histories experimentally determined in the sample (workpiece) to calculate the corresponding input heat flux for a given set of system parameters. In this work, golden section method is used (Vanderplaats, 1999). It means, the values of q_i will be supposed to be those that minimize Eq. (10). This procedure requires that the estimated temperature $T(r_j, t_i, q_i)$, j=1,2,...M, computed from the solution of direct problem, Eq.(10), by using the estimated values of the components q_i, i=1,2,..M, should match the measured temperature $Y(r_j,t_i)$ as closely as possible for each instant t_i.

The optimization technique used assures that the value of q_0" (Eq. 13) is replaced by the minimum value found in this interval. The optimization technique used is the one-dimensional golden section method. The objective function, in this case, is the estimator given by Eq. (17) that is minimized between the lower and upper bounds, q_l and q_u , respectively. The golden section method for estimating the maximum, minimum, or zero of a one-variable function is a popular and well-known technique. To determine the minimum of a function (Eq.17) this method only needs to know the lower q_l and upper q_u bounds of the parameter which bracket the minimum. The function F_q is assumed to be unimodal and the minimum value is found in this interval by an iterative process when a desired tolerance is reached. More details of this method can be found in Vanderplaats, (1999).

3. RESULTS

3.1. Simulated tests

In order to verify the inverse technique a simulated case test is analyzed before its application in an experimental test. In this sense, temperature distribution for the direct problem are generated considering a known heat flux evolution $q_0^{"}$. Random errors are then added to these temperatures. The temperatures with error are then used in the inverse algorithm to reconstruct the imposed heat flux. The simulated temperature are calculated as

$$Y(L,t) = T(L,t) + \varepsilon_j . \tag{27}$$

where ε_j is a random number. The parameter ε_j assumes values of 0, ± 5°C .

The validity for this test can be assured through the comparison between the temperature calculated and measured at rake face. Figure 2 show this comparison for thermocouples 1 located at position x=100mm, y=25mm, z=4 mm.

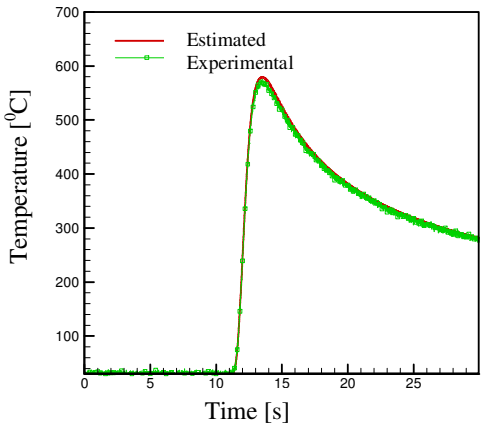

Fig. 2. Comparison between the temperature calculated and measured at rake face.

The temperature evolution during the simulated welding can be shown in Fig. 3

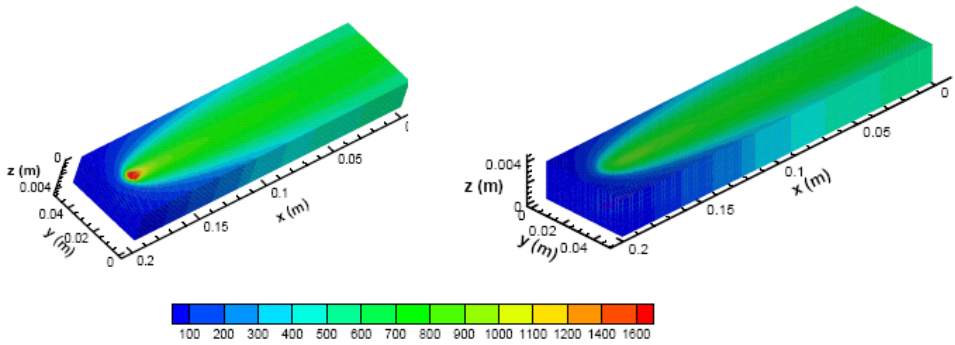

Figure 3. Resulting temperature field at the welding face at different elapsed welding times. a) Frontal view of the workpiece; b) the opposite face to the welding process.

3.2. Experimental test

The welding gun, which represents the point heat source, moves at a specific speed along a straight path by using a totally automated X-Y coordinate table. To avoid dimension interference, the test-plate is held in air by 4 end pointed cylindrical screws, so that, only a small contact area exists. A set of experiments was carried out on AISI 304 stainless steel test plates with dimensions of 200x50x4 mm, using the following welding setting conditions: direct polarity (CC-), current at 78A, arc length (distance from the electrode top to the plate surface) adjusted to 4 mm, shielding gas (Ar and Ar+25%He). The electrode used was a 1.6 mm of diameter, AWS EWTh-2 (tungsten doped with 2% of thory) with an included angle of 60^o. The shielding gas flow was set at 8 l/min (0.133 10^{-3} m^3/s) and the welding speed at 0,005m/s. The resultant arc voltage was monitored around 15 V. The values of the thermal properties of the AISI 304 as a function of temperature were obtained from literature (Gonçalves, 2006). The values of the thermal properties of the AISI 304 as a function of temperature as

$$k = 14.42 + 0.0169\,T - 2.44\times10^{-6}\,T^2\ W/mK \quad c_p = 486.6 + 0.159\,T + 18.07\times10^{-6}\,T^2\ W/kgK$$

and T_m = 1700K and

The welding is carried out on a plane position with the bead on plate technique. Two independent data acquisition systems are used. In the first one, a data acquisition chart is used to monitor the voltage and current signals at 12 bits and 10 kHz per channel. The second one is composed by a microcomputer-based data acquisition system (HP 75000 B E1326B), DAS for short, is used in order to acquire and store the thermocouple data. The DAS, under a software control, sampled (multiplexed) each thermocouple signal at intervals of 0.38 s (totaling 1028 points for each thermocouple).

Ten thermocouples are used. They are located at the opposite face of the weld. Table 1 presents the exact positions of the thermocouples. Once the heat flux to the workpiece is estimated, the temperature distribution can be obtained

solving the direct problem given by Eq. (21). Figure 4 presents three views of temperature field at the instant of 20 s in order to visualize the weld pool and the depth of weld penetration.

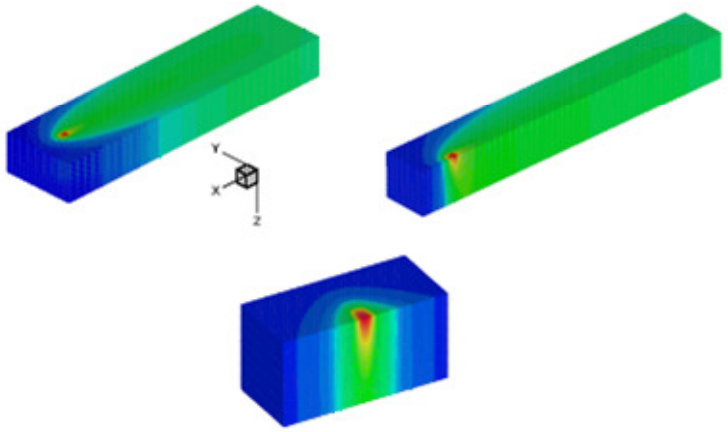

Figure 6. Three-dimensional presentation of temperature distribution in the test-plate at instant of 35 s.

.

Table 1. Thermocouple positions on the workpiece (according to Fig. 1).

Position/Thermocouple	1	2	3	4	5	6	7	8	9	10
X [mm]	13.28	30.88	46.22	63.00	79.88	95.02	112.80	128.72	146.26	160.82
Y [mm]	25.00	35.00	25.00	35.00	25.00	35.00	25.00	35.00	25.00	35.00
Z [mm]	4.0	4.0	4.0	4.0	4.0	4.0	4.0	4.0	4.0	4.0

Figure 5 shows the comparison between the estimated and experimental temperatures for the five thermocouples. One can see a satisfactory agreement. The deviations can be attributed to various factors besides the common experimental difficulties or to the thermal properties values used in the theoretical model due to the mettalic phase changes.

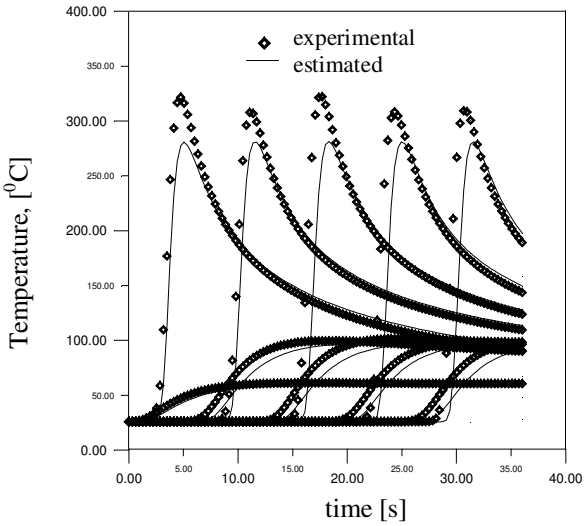

Figure 5 Comparison between estimated and experimental temperatures at the opposite face of the welding bead

4. CONCLUSIONS

The theoretical and experimental approach, based on the application of the Golden Section Inverse Technique, showed to be a promising tool for calculating the thermal history experimented by a workpiece under welding. The three-dimensional model based on enthalpy method seems to be a satisfactory model. However the model is strongly dependent of precise thermal properties values what must be known to obtain precise results. In this sense, the agreement between the predicted temperature and the measured temperature are quite satisfactory, what leads for the reasoning that the estimated values for heat flux are reliable.

5. ACKNOWLEDGEMENTS

The authors would like to thank FAPEMIG (Proc. Tec 00166/06) and CNPq for the financial support without which this work would not be possible.

6. REFERENCES

Alifanov, O. M., 1975, " Solution of na Inverse Problem of Heat Conduction by Iterations Methods", *Journal of Engineering Physics, **10***.

Al-Khalidy, Nehad, 1995, "Enthalpy Technique for Solution of Stefan Problems: Application of the Keyhole Plasma Arc Welding Process involving moving heat source", Int. Comm. Heat Mass Transfer 22, pp.779-790.

Al-Khalidy, Nehad, 1997, "Application of Optimization Methods for Solving Inverse Phase-Change Problems, Numerical Heat, part B, pp. 477-497.

Beck,J.V., Blackwell, B. Clair, C.R. St., 1985, "Inverse Heat Conduction, Ill-posed Problems", Wiley Interscience Publication, New York

Bonifaz, E.A. , 2000, "Finite Element Analysis of heat Flow in Single-Pass Arc Welds"**,** Welding Research Supplement, pp.121-125.

Cao, Y., Faghri, A., and Chang, W., 1989, " A Numerical Analysis of Stefan Problems for Generalized Multi-Dimensional Phase-Change Structures Using the Enthalpy Transforming Model", Int. Journal of Heat and Mass Transfer, Vol. 32, No. 7, pp.1289-1298.

Crank, John, 1984, "Free and moving boundary problems", Claredon Press, Oxford University Press, New York, United States.

Gonçalves, C. V., Vilarinho, L. O., Scotti, A., Guimarães, G., 2006. Estimation of heat source and thermal efficiency in GTAW process by using inverse techniques. Journal of Materials Processing Technology. 172, 42-51.

Hsu, Y. e Rubinsky, B., 1988, "Two Dimensional Heat Transfer Study on the Keyhole Plasma Arc Welding Process", Int. Journal of Heat and Mass Transfer, Vol. 31, No. 7, pp. 1409-1421.

Hsu, Y. F., Rubinsky, B., and Mahin, K., 1986, "An Inverse Finite Element Method for the Analysis of Stationary Arc Welding Processes", Journal of Heat Transfer, vol. 108, pp. 734-741.

Incropera, F. P. e DeWitt, D. P., 1998, "Fundamentos de transferência de calor e de massa", LTC – Livros Técnicos e Científicos Editora S. A., Rio de Janeiro, RJ, Brasil.

Katz, M. e Rubinsky, B., 1984, "An Inverse Finite – Element Technique to Determine the Change of Phase Interface Location in One – Dimensional Melting Problems ", Numerical Heat Transfer, Vol.7, pp. 269 – 283.

Nedjar, B., 2002, "An Enthalpy-based Finite Element Method for Nonlinear Heat Problems Involving Phase Change", Computers and Structures, Vol. 80, pp. 9-21.

Nguyen, T. Ohta, A. Matsuoka, K. Suzuki, N. Maeda, Y. , 1999, "Analytical Solutions for Transient Temperature of Semi-Infinite Body Subjected to 3-D Moving Heat Sources", Welding Journal, pp. 265-274

Patankar, S.V. , 1980, "Numerical Heat Transfer and Fluid Flow", Hemisphere Publishing Corporation, USA, 1980.

Pretot, S., Zeghmati, B., Caminat, Ph., 2000. Influence of surface roughness on natural convection above a horizontal plate. Advances in Engineering Software. 31, 793-801.

Rosenthal, D., 1941, "Mathematical theory of heat distribution during welding and cutting", Welding Journal 20, pp. 220-234.

Rubinsky, B., e Shitzer, A., 1978, " Analytic Solutions to the Heat Equation Involving a Moving Boundary With Applications to the Change of Phase Problem (the Inverse Stefan Problem)", Journal of Heat Transfer, Vol. 105, 1983, pp. 550 – 554.

Tsai, C.L. . Hou, C.A , 1988, "Theoretical Analysis of Weld Pool Behavior in the Pulsed Current GTAW Process"**,** Journal of Heat Transfer 110, pp. 160-165.

Vanderplaats,, G.N, 1999, "Numerical Optimization Techniques for Engineering Design", McGraw-Hill, USA

Voller, V. R., e Prakash, C., 1987, A fixed grid numerical modeling methodology for convection/diffusion mushy region phase change problems", International Journal of Heat and Mass Transfer, Vol. 30, No. 8, pp. 1709-1719.

7. RESPONSIBILITY NOTICE

The author(s) is (are) the only responsible for the printed material included in this paper.